Water and Trehalose: How Much Do They Interact with Each Other?

S. E. Pagnotta,[†] S. E. McLain,[‡] A. K. Soper,[¶,§] F. Bruni,*[,∥] and M. A. Ricci[∥]

Centro de Fisica de Materiales (CSIC-UPV/EHU) MPC, 20008 Donostia-San Sebastian, Spain, School of Health and Biomedical Sciences, King's College London, London SE1 9NH, U.K., Isis Facility, STFC Rutherford Appleton Laboratory, Chilton, Didcot OX11 0QX, U.K., Department of Physics and Astronomy, University College London, London WC1E 6BT, U.K., and Dipartimento di Fisica "E. Amaldi", Università degli Studi "Roma Tre", 00146 Roma, Italy

Received: December 17, 2009; Revised Manuscript Received: March 2, 2010

The observation made by early naturalists that some organisms could tolerate extreme environmental condisions and "enjoy the advantage of real resurrection after death" [Spallanzani, M. *Opuscules de Physique Animale et Vegetale* **1776** (translated from Italian by Senebier, J. *Opuscules de Physique Animale et Vegetale* **1787**, *2*, 203−285)] stimulated research that still continues to this day. Cryptobiosis, the ability of an organism to tolerate adverse environments, such as dehydration and low temperatures, still represents an unsolved and fascinating problem. It has been shown that many sugars play an important role as bioprotectant agents, and among the best performers is the disaccharide trehalose. The current hypothesis links the efficiency of its protective role to strong modifications of the tetrahedral arrangement of water molecules in the sugar hydration shell, with trehalose forming many hydrogen bonds with the solvent. Here, we show, by means of state-of-the-art neutron diffraction experiments combined with EPSR simulations, that trehalose solvation induces very minor modifications of the water structure. Moreover, the number of water molecules hydrogen-bonded to the sugar is surprisingly small.

Introduction

It has long been known that some organisms can withstand severe environments and have the ability to experience what early naturalists termed "real resurrection after death".[1] For instance, the ability of organisms to survive in conditions which result in the almost total loss of intracellular water (anhydrobiosis) still represents an unsolved and fascinating problem. Often, these extreme conditions are attributable to the availability or temperature of water as, similarly, the ability to withstand freezing temperatures avoiding ice formation is observed in several organisms and has important applications related to the cryopreservation of biomaterials. Many sugars play an important role as bioprotectant agents; among the best performers is the disaccharide trehalose, and there is a general consensus in the literature on the peculiar role and properties of trehalose, compared to other sugars, as a stabilizer and protective agent against environmental stresses.

Trehalose is naturally produced by several organisms that are able to survive severe environmental conditions, such as drought or extreme temperatures.[2−6] The origin of the beneficial role of trehalose should reside in the mechanism of its interaction with enzymes, other molecules of biological relevance, and biomembranes which are preserved against stressing conditions when embedded in trehalose matrixes.[7−10] Although knowledge of the detailed manner in which carbohydrates, and in particular trehalose, stabilize macromolecules and biomembranes remains incomplete; it is clear that water should play an important role in determining their physical and chemical stability. These observations have stimulated intensive research[11−13] on the dynamical and structural properties of water in trehalose−water systems as a function of solute concentration and temperature. In particular, the nature and the extent of the interaction between trehalose and water and a detailed understanding of the reasons that make trehalose special compared to the other carbohydrates remain still open issues. The microscopic structure of trehalose−water solutions has been investigated by nuclear magnetic resonance (NMR) studies, looking in particular at the conformation of trehalose in solution.[14] However, while NMR is a remarkable technique for determination of conformation in solution, it yields no structural information about the hydrogen bonding (HB) network between solutes and the solvent through their exchangeable hydrogen sites. Similarly, a number of dynamical studies using IR and Raman spectroscopy, terahertz absorption measurements, and neutron scattering have inferred the structural properties of trehalose in aqueous solution.[15−19] In particular, the presence of trehalose is supposed to distort or break the hydrogen bond network of water due to a strong interaction between water and trehalose. However, while there is compelling evidence on the dynamical properties of water in a trehalose solution as being different from those of neat water, structural properties from these investigations can only be inferred as dynamical measurements do not provide a direct assessment of the structure of the system. Although dynamical measurements can greatly enhance our understanding of a liquid, it is not straightforward, and maybe not even reliable, to determine structural information from these investigations. Similarly, structural measurements such as those presented here do not give information concerning the energetics present in solution, such as the distribution of the H bond stretching modes between water molecules. Several computational studies have looked at the trehalose−water solution and shown a disruption of the

* To whom correspondence should be addressed. E-mail: bruni@fis.uniroma3.it.
[†] Centro de Fisica de Materiales (CSIC-UPV/EHU).
[‡] King's College London.
[¶] STFC Rutherford Appleton Laboratory.
[§] University College London.
[∥] Università degli Studi "Roma Tre".

10.1021/jp911940h
Published on Web 03/18/2010

tetrahedral arrangement of water molecules near the disaccharide due to steric constraints imposed by the solute and its ability to form stable hydrogen bonds with proximal water molecules.[20–23] Nevertheless, a comparison between the results of these computational studies and experimental findings is severely limited due to lack of complete and direct experimental studies of the microscopic structure of water in trehalose solutions.

Here, we show the results of a structural analysis of a water−trehalose solution at two concentrations, looking in particular at the proximal water molecules likely involved in hydrogen bonding to specific trehalose sites and at the perturbation of water tetrahedral coordination compared to neat water. Neutron diffraction is a suitable probe for the structural study of aqueous solutions due to the large scattering cross section of deuterium and the high contrast achievable upon H/D selective substitution on all exchangeable hydrogen sites in the solution. Therefore, the main goal of this work was to obtain high-quality structural data that can allow a microscopic investigation of the interactions between water and trehalose. This has been accomplished by supplementing the isotopic substitution neutron diffraction experiments with computer modeling, as described in the following section.

Materials and Methods

Neutron diffraction with isotopic substitution (see, for instance, ref 24) allows labeling of individual atomic sites and the extraction of selected pair radial distribution functions (RDF), $g(r)$, by combining different data sets. Each RDF represents the probability of finding an atom at a given r distance from the other atom of the pair. Neutron diffraction experiments with isotopic H/D substitution[24] have been performed on trehalose aqueous solutions, at concentrations of 1 solute per 100 water molecules and 1 solute per 25 water molecules (equivalent to 16 and 43 wt %), at standard temperature and pressure ($T = 298$ K, $p = 1$ bar), aimed at investigating the presence of water−trehalose HB along with the influence of this disaccharide on the HB network of water. The experiment has been performed by exploiting the H/D isotopic substitution on the water hydrogens and on the exchangeable proton sites of trehalose. The data have been analyzed according to the procedure described below and transformed in r space by implementing a Monte Carlo simulation, which fits the experimental data.[29–31] At the lowest solute concentration, protonated trehalose (H-trehalose) has been solvated in pure D_2O, pure H_2O, and a 50 mol % mixture of the two (hereafter labeled as HDO). At the highest concentration, five more samples have been prepared by using a partially deuterated trehalose sample (D-trehalose), prepared by several hydration and dehydration processes in D_2O, leading to exchange of all exchangeable hydrogens; these trehalose solutes have been solvated in D_2O, H_2O, and HDO. Finally, a 50 mol % mixture of H-trehalose and D-trehalose has been solvated in D_2O and HDO, making a total of eight samples at this concentration. Measurements have been carried out at the SANDALS[25] diffractometer, installed at the ISIS Facility[26] (U.K.). Standard 1 mm Ti−Zr sample containers and the SANDALS sample changer connected to a water bath have been used. In addition to the measurement of the samples, data were collected on the background scattering, empty containers, and vanadium sample, used for putting the data on an absolute scale of scattering cross section.

Diffraction data have been analyzed by using the Gudrun suite of programs, which performs corrections for multiple scattering, absorption, and inelasticity effects, along with subtraction of the scattering from the sample container and data reduction to an absolute scale.[27] The outputs of Gudrun are the total neutron-weighted interference differential cross sections (IDCS) defined as

$$F(Q) = \sum_{\alpha} \sum_{\beta \geq \alpha} w_{\alpha\beta}[S_{\alpha\beta}(Q) - 1] \qquad (1)$$

where Q is the exchanged wave vector, α and β label the atomic sites, and

$$S_{\alpha\beta}(Q) = 4\pi\rho \int_0^{\infty} r^2(g_{\alpha\beta}(r) - 1) \frac{\sin(Qr)}{(Qr)} \mathrm{d}r \qquad (2)$$

called the partial structure factor (PSF), is the Fourier transform of the RDF, $g_{\alpha\beta}(r)$, where ρ is the atomic number density of the solution in question. The individual PSFs are weighted in eq 1 by $w_{\alpha\beta} = c_\alpha c_\beta b_\alpha b_\beta (2 - \delta_{\alpha\beta})$, where c_α and c_β are the concentration of the α and β nuclei and b_α and b_β their scattering lengths,[28] respectively. Thus, each experimental IDCS is a linear combination of many PSFs, and in order to extract from the available experimental data information on the individual site−site RDF, direct Fourier transform of the IDCS or of combinations of the experimental data is of limited usefulness. In liquids with a small number of distinct atoms, like H_2O, by measuring an array of different isotopically labeled samples, it is possible to directly extract all of the pair correlation functions from the experiment, giving a direct assessment of the hydrogen bonding present in the measured liquid. However, in more complex solutions, it is not possible to istopically label every atom site; for this reason, we employ a simulation-assisted procedure that has been developed in the past decade in order to convert IDCS data to real space, with extraction of the whole set of RDFs. This is called empirical potential structure refinement (EPSR)[29–31] and is similar in principle to the methods routinely used in crystallography, which attempt to systematically refine a structural model to give best overall agreement with the diffraction data. This method is currently the most informative available for refining these structures in the liquid state. Moreover, it should be noted that as many isotopic contrasts as possible are measured; EPSR is constrained to fit all of the data sets, ensuring a physically reasonable model which is consistent with measured diffraction data at the appropriate density and composition of the measurement.

The EPSR method builds a simulation box with the same density and composition as the real sample. It does this by means of a reference interaction potential, U_{ref}, which incorporates the distinctive characteristics of the system in question (such as molecular structure and, for instance, the possible presence of H bonds between water molecules and between the solute and solvent) and is used to seed a Monte Carlo simulation. Once this has reached equilibrium, a perturbation to the reference potential, called the empirical potential, derived directly from the diffraction data, is introduced and used to drive the simulated diffraction patterns as close as possible to the measured data. Since the fit of diffraction data is derived directly from the pair correlation function, this empirical potential is by definition purely pairwise-additive. The Monte Carlo simulation proceeds using both the reference potential and the empirical potential to accept or reject moves, and the empirical potential is adjusted iteratively until the fit to the data cannot be improved further. This method allows calculation of structural quantities beyond the RDF, as in any simulation work; it can also help to identify any systematic bias that may affect one or more data sets when

TABLE 1: Sample Density, Simulation Box Size, and Number of Water and Trehalose Molecules in the Simulation Box for the Two Samples Examined

sample	density (atoms/Å ^{3})	L_{box} (Å)	H_2O	trehalose
1:25	0.025	27.37	500	20
1:100	0.030	32.21	1000	10

TABLE 2: Parameters of the Lennard-Jones Potential and Fractional Charges Used in the Reference Potential Model, U_{ref}, to Start the EPSR Simulations

atom	ε (kJ/mol)	σ (Å)	q (e)
O_w	0.65	3.166	−0.8476
H_w	0.0	0.0	0.4238
O_1	0.58576	2.9	−0.5
O_2	0.58576	2.9	−0.5
O_3	0.71128	3.1	−0.5
O	0.71128	3.1	−0.5
H	0.05	1.7	0.3005
M	0.12552	1.7	0.0
C	0.27614	3.5	0.258

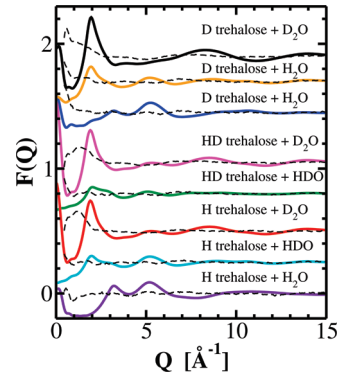

Figure 1. Neutron interference differential cross section, $F(Q)$, for all H/D-substituted samples at a concentration of 1 trehalose per 25 water molecules. The black dashed lines are the EPSR fit residuals, which do not show physical structures but only a slowly decaying baseline due to residual systematic errors, which affect the radial distribution functions at distances shorter than the minimum approach distances between atomic pairs. The quality of the fit at the lowest trehalose concentration is the same.

features in the data not compatible with physical configurations of molecules are found.

At each trehalose concentration, a simulation box has been prepared according to data reported in Table 1 in order to match the experimental density and composition of the samples. Water sites have been labeled as O_w and H_w, and in order to restrict the number of sites on the trehalose molecule, all carbons have been labeled as C; all nonexchangeable hydrogen sites are labeled as M and the exchangeable ones as H; the oxygen at the α 1−1 glycosidic bond is labeled as O_1, the saccharide ring oxygens (one per ring) as O_2, oxygen of the hydroxyl groups ending the CH_2OH side chains (one per ring bonded to the C_6 site) as O_3, and all other oxygens as O (see Table 2 and Figure 2). Each ring of the trehalose molecule is allowed to rotate around the glycosidic bond. Each CH_2OH side chain can rotate around the C−C bond. Moreover, each bond in the water and in the trehalose molecule is not rigid, and a degree of flexibility is included in the EPSR procedure. The simple point charge/extended (SPC/E) model[32] has been used as a reference potential for water, and Lennard-Jones centers plus charges (see Table 2 for the parameters) have been used to simulate the interaction between trehalose sites. The Lorentz−Berthelot rules have been applied to describe the interaction between different atoms.

The quality of the best fit achieved running the EPSR simulation can be appreciated by looking at Figure 1, where the data and fit residuals are shown for all data sets.

Results and Discussion

We have identified four distinct sites on the trehalose molecule, which are, in principle, good candidates for HB with water; these are labeled according to Figure 2 and 2A and consist of two distinct hydroxyl groups, namely, OH and O_3H, along with two distinct oxygen sites (O_1 and O_2).

There is evidence for hydrogen bonding at both O_1 and O_2 sites; the RDFs which describe their hydration (Figure 2B) show one peak at a distance of ∼1.74 Å due to O_1H_w and O_2H_w correlations and a peak at about 2.7 Å due to O_1O_w and O_2O_w correlations. In all of these functions, the peaks move to larger distances (for instance, 1.81 instead of 1.74 Å for the OH_w correlations) with decreasing trehalose concentration, while the peak intensity increases so that the average number of hydrogen bonds is lower than 1 at each site, irrespective of concentration. This means that, on average, there are between two and three hydrogen-bonded water molecules per trehalose molecule at these sites, independent of the trehalose concentration. These molecules are likely the so-called internal water molecules which are responsible for the folding of the molecule by bridging between the O_1 and O_2 sites and other oxygens on the glucose ring. Interestingly, folding due to water-mediated intramolecular H bonding is assumed to be one of the trehalose strategies for counteracting the scarcity of water by trapping these internal water molecules.[21] In addition, the $g_{OH_w}(r)$ and $g_{O_3H_w}(r)$ functions (Figure 2A) show a peak at a distance compatible with hydrogen bonding (namely, at 1.97−1.98 Å), although with very low intensity. However, in a trehalose molecule, there are two O_3 sites and six O sites, according to our labeling; therefore, on average, there is one water molecule bonded at one O_3 site and close to two water molecules bonded at one of the O sites per trehalose molecule. All of the O-labeled oxygen sites in our scheme (Figure 2A) are hydroxyl oxygens and are therefore covalently bonded to a hydrogen atom. Surprisingly, the data here show that these hydrogens do not form strong hydrogen bonds with the surrounding water molecules; the $g_{HO_w}(r)$ functions (Figure 2C) show a very broad, although structured, peak starting at ∼2 Å and extending up to 4.4 Å. Therefore, there is no clear indication of a hydrogen bond formed at the H sites at both trehalose concentrations.

Comparison with previous determinations of the water−trehalose RDFs can only be performed on selected functions calculated by computer simulations. For instance, the g_{OO_w} and $g_{O_2O_w}$ available in the literature[21] are in fair agreement with our data. Even though the trehalose concentrations investigated in the present study (16 and 43%) and in the computational study cited above (6%) are quite different, this should not hinder the comparison as the correlation between a trehalose site (either O or O_2) with a proximal water oxygen does not depend on the number of water molecules in solution, most of them being at a larger distance from the solute. However, the comparison may be biased since that simulation[21] was performed with a system made up by a single trehalose and 300 water molecules; this has at least an obvious effect on the low r range of the RDF, where our data show a slope due to regions of the sample occupied by other trehalose molecules and thus not accessible to water molecules (excluded volume effects).

Although the number of water molecules in the first hydration shell of trehalose is as high as that expected for such a large

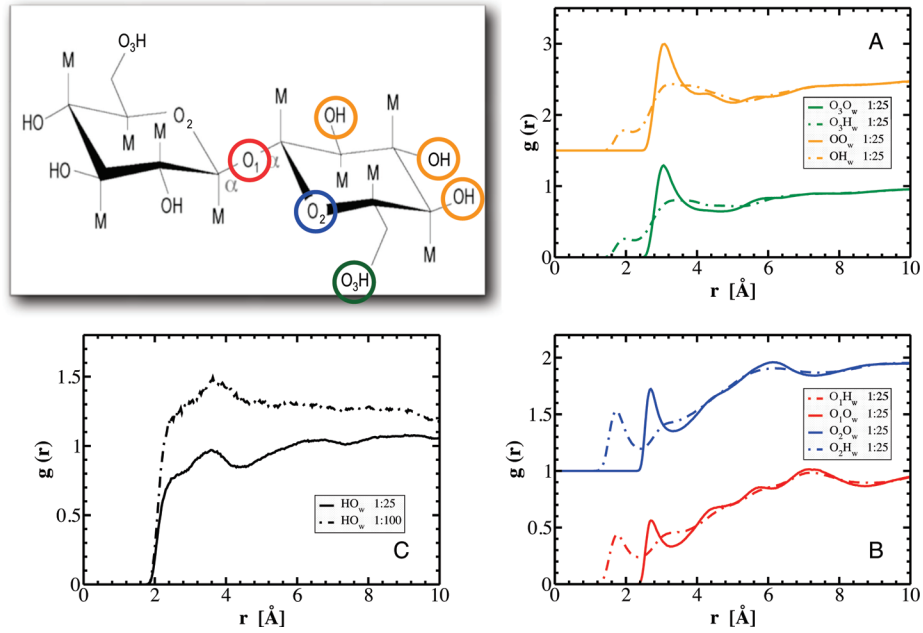

Figure 2. Structural formula of trehalose and selected trehalose−water radial distribution functions. Trehalose is a disaccharide formed by an α 1−1 glycosidic bond between two glucose molecules, at site O_1. M sites label nonexchangeable hydrogens and H the exchangeable ones; OH labels the hydroxyl groups bonded to each ring carbon (three per ring, circled in orange); O_2 labels the saccharide ring oxygens (one per ring, circled in blue); and O_3H are the hydroxyl groups ending the CH_2OH side chains (one per ring bonded to the C_6 site and circled in green). The same color code is adopted in (A) and (B) to identify the radial distribution functions of these sites with water oxygens, O_w, (solid) and hydrogens, H_w, (dot−dashed). (C) The radial distribution functions of the exchangeable H sites with water oxygens at concentrations of 1:25 (solid) and 1:100 (dot−dashed) trehalose to water molecules.

molecule (for instance, each O site has about four neighboring water molecules within a distance on the order of 4 Å), only between three and five water molecules are H-bonded to the trehalose molecules, and two or three of them may be identified as internal.

The second issue concerns the disturbance brought on by trehalose solvation to the HB network of water. In contrast with previous literature,[23] we do not see evidence for large distortions or breaking of the HB network. The water−water RDF for the less concentrated trehalose solution are quite similar to those of neat water, while at the highest concentration investigated, a clear, although small, shift to shorter distances of the peaks can be observed (Figure 3A). In particular, at both concentrations, the second peak of the O_wO_w radial distribution function shifts inward and is broader compared to that of pure water. This peak, when centered at ∼4.5 Å, is indeed considered the signature for a tetrahedral arrangement of water molecules and moves to shorter distances in the presence of various solutes[33] or with increasing external pressure,[34] while very high temperatures are needed to move it toward higher distances.[35] The shift of this peak at both trehalose concentrations investigated is much smaller than that observed with similar salt concentrations and is much less concentration-dependent. Moreover, we remark that the increase of peak intensity observed in all site−site RDFs at high solute concentration is a trivial effect of the consequential lower water concentration and cannot be taken as a signal for increased sugar hydration, as is sometimes reported.[36] To confirm this point, we have calculated the coordination number, $n_{O_wO_w}(r)$, namely, the number of water oxygens at a given distance r from a central water molecule, plotted in Figure 3B. It can be seen that in the region of the first peak of the oxygen−oxygen RDF, at around 3 Å, the coordination number is between 3 and 4, as in the case of neat water.

Finally, the state of the HB network can be investigated by looking at the HB distribution function (Figure 4). Changes with increasing trehalose concentration are limited to a decrease of the number of water molecules forming three hydrogen bonds, with a consequential increase of the number of monomers. These changes, however, leave the average number of bonds per molecule almost unchanged, between 3.5 and 3.4 bonds per molecule, to be compared with 3.8 for pure ambient water. Moreover, assuming a binomial distribution, the probability that a molecule forms a hydrogen bond can be calculated from the number of water molecules engaged in four hydrogen bonds, giving at both concentrations $p_{HB} = 0.8$. This value implies, according to the percolation theory,[37] that water molecules form a fully percolating HB network independent of the trehalose concentration. This suggests that the number of monomers increases at the expense of the water molecules' first neighbors of the trehalose, without fragmenting the HB percolating cluster.

In conclusion, our study suggests that H bonding between trehalose and water is surprisingly limited, given the large number of sites on the trehalose molecule that, in principle, could interact with water. In addition, the influence of trehalose solvation on the water network is also surprisingly small. These conclusions are at odds with the accepted view that considers strong water−trehalose interactions (namely, a large number of hydrogen bonds and severe modifications of water structure) as a key fact to explain the ability of trehalose to protect biological molecules from extreme temperatures and dehydration. A large number of hydrogen bonds and strong water structure modifications were suggested by computer simulations and/or experimental studies probing sample dynamics, as discussed in the Introduction. Computer simulations in the absence of constraining data are solely dependent on the interaction potentials or force fields used for the simulation and, as such, may not easily be able to discern structural details of the system in question. Similarly, extrapolation of structural information from dynamical experiments such as IR and Raman is not very precise, and changes in the dynamics of any give

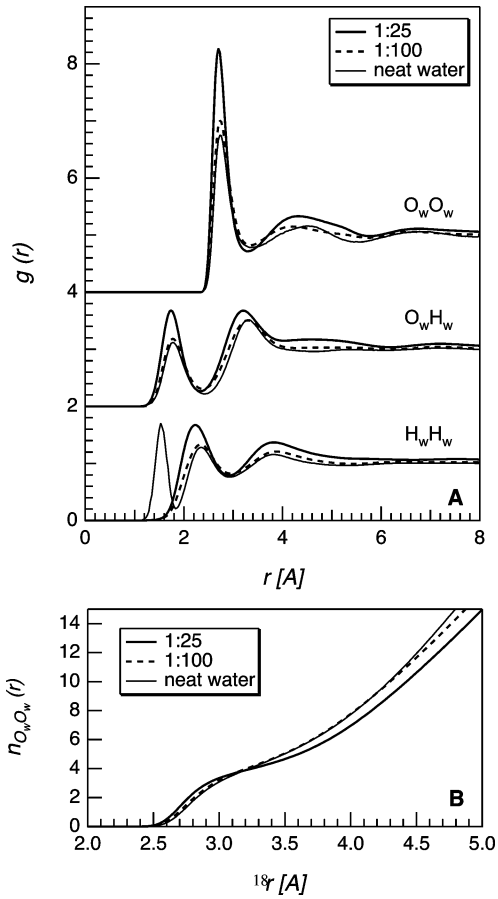

Figure 3. (A) The water−water radial distribution functions at the two investigated concentrations; H_wH_w, O_wH_w, and O_wO_w, shifted from bottom to top. The same functions for pure ambient water are reported as thin solid lines; these latter functions contain also the intramolecular H_wH_w peak at ∼1.55 Å and the O_wH_w at ∼1 Å. (B) Running coordination numbers for water oxygens.

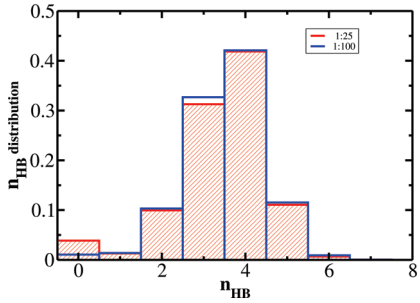

Figure 4. The distribution function of the number of water−water hydrogen bonds at a concentration of 1 trehalose per 25 water molecules (red dashed) and of 1 trehalose per 100 water molecules (blue).

system could easily be consistent with a large range of different structural motifs. Although spectroscopic techniques are reliable probes for intramolecular and local dynamic order, such as bond stretching and bending, they cannot easily be directly connected to intermolecular bonding structure in solution and do not give any information on how, for instance, a water molecule does or does not bond to trehalose in solution. We remind the reader that the present experiment is the first direct and thorough study of the microscopic structure of water−trehalose solutions. At this stage, we could speculate that the protective effect provided by trehalose to biomolecules and biostructures may not be entirely water-mediated. Indeed, a large fraction of first-neighboring water molecules are only loosely coordinated, thus leaving trehalose available for direct H bonding with other solutes.

Acknowledgment. This work has been performed within the Agreement No. 06/20018 between STFC and CNR, concerning collaboration in scientific research at the spallation neutron source ISIS, and with partial financial support of CNR. S.E.P. acknowledges financial support of CNISM during the experiment.

References and Notes

(1) (a) Spallanzani, M. *Opuscules de Physique Animale et Vegetale* 1776. Translated from Italian by (b) Senebier, J. *Opuscules de Physique Animale et Vegetale* **1787**, *2*, 203−285.
(2) Crowe, J. H.; Clegg, J. S. In *Dry Biological Systems*; Academic Press: New York, 1978.
(3) Crowe, J. H.; Crowe, L. M.; Jackson, S. A. *Arch. Biochem. Biophys.* **1983**, *220*, 477.
(4) Crowe, J. H.; Crowe, L. M.; Chapman, D. *Science* **1984**, *223*, 701.
(5) *Membranes, Metabolism, and Dry Organisms*; Leopold, A. C., Ed.; Cornell University Press: Ithaca, NY, 1986.
(6) Crowe, L. M. *Comp. Biochem. Physiol.* **2002**, *131*, 505.
(7) Carpenter, J. F.; Crowe, J. H. *Biochemistry* **1989**, *28*, 3916.
(8) Crowe, J. H.;, Crowe, L. M. In *Liposomes, New Systems and New Trends in their Applications*; Pusieux, F., et al., Eds.; Editions de Sante: Paris, 1995; pp 237−272.
(9) Sampedro, J. D.; Uribe, S. *Mol. Cell. Biochem.* **2004**, *256−257*, 319.
(10) Chiantia, S.; Giannola, L. I.; Cordone, L. *Langmuir* **2005**, *21*, 4108.
(11) Belton, P. S.; Gil, A. M. *Biopolymers* **1994**, *34*, 957.
(12) Allison, S. D.; Chang, B.; Randolph, T. W.; Carpenter, J. F. *Arch. Biochem. Biophys.* **1999**, *365*, 289.
(13) Cordone, L.; Cottone, G.; Giuffrida, S. *J. Phys.: Condens. Matter* **2007**, *19*, 205110.
(14) Batta, G.; Kover, K. E.; Gervay, J.; Hornyak, M.; Roberts, G. M. *J. Am. Chem. Soc.* **1997**, *119*, 1336.
(15) Branca, C.; Magazú, S.; Maisano, G.; Bennington, S. M.; Fåk, B. *J. Phys. Chem. B* **2003**, *107*, 1444.
(16) Lerbret, A.; Bordat, P.; Affouard, F.; Guinet, Y.; Hédoux, A.; Paccou, L.; Prévost, D.; Descamps, M. *Carbohydr. Res.* **2005**, *340*, 881.
(17) Magazù, S.; Migliardo, F.; Ramirez-Cuesta, A. J. *J. R. Soc. Interface* **2007**, *4*, 167.
(18) Heyden, M.; Bründermann, E.; Heugen, U.; Niehues, G.; Leitner, D. M.; Havenith, M. *J. Am. Chem. Soc.* **2008**, *130*, 5773.
(19) Dashnau, J. L.; Conlin, L. K.; Nelson, H. C. M.; Vanderkooi, J. M. *Biochim. Biophys. Acta* **2008**, *1780*, 41.
(20) Bonanno, G.; Noto, R.; Fornili, S. L. *J. Chem. Soc., Faraday Trans.* **1998**, *94*, 2755.
(21) Conrad, P. B.; de Pablo, J. J. *J. Phys. Chem. A* **1999**, *103*, 4049.
(22) Lawrence Lee, S.; Debenedetti, P. G.; Errington, J. R. *J. Chem. Phys.* **2005**, *122*, 204511.
(23) Lerbret, A.; Bordat, P.; Affouard, F.; Descamp, M.; Migliardo, F. *J. Phys. Chem. B* **2006**, *109*, 11046.
(24) Botti, A.; Pagnotta, S. E.; Bruni, F.; Ricci, M. A. *J. Phys. Chem. B* **2009**, *113*, 10014.
(25) Soper, A. K. In *Proceedings of the Conference on Advanced Neutron Sources 1988*, IOP Conf. Proc. no. 97; Hyer, D. K., Ed.; Institute of Physics and Physical Society: London, 1989; pp 353−366.
(26) Science and Technology Facilities Council. www.isis.rl.ac.uk (2010).
(27) Disordered Materials Homepage. http://www.isis.stfc.ac.uk/groups/disordered-materials/disordered-materials-6252.html (2010).
(28) Sears, V. F. *Neutron News* **1992**, *3*, 26.
(29) Soper, A. K. *Chem. Phys.* **1996**, *202*, 295.
(30) Soper, A. K. *Chem. Phys.* **2000**, *258*, 121.
(31) Soper, A. K. *Mol. Phys.* **2001**, *99*, 1503.
(32) Berendsen, H. J. C.; Grigera, J. R.; Straatsma, T. P. *J. Phys. Chem.* **1987**, *91*, 6269.
(33) Mancinelli, R.; Botti, A.; Bruni, F.; Ricci, M. A.; Soper, A. K. *Phys. Chem. Chem. Phys.* **2007**, *9*, 2959.
(34) Soper, A. K.; Ricci, M. A. *Phys. Rev. Lett.* **2000**, *84*, 2881.
(35) Jedlovszky, P.; Brodholt, J. P.; Bruni, F.; Ricci, M. A.; Soper, A. K.; Vallauri, R. *J. Chem. Phys.* **1998**, *108*, 8528.
(36) Ekdawi-Server, N. C.; Conrad, P. B.; de Pablo, J. J. *J. Phys. Chem. A* **2001**, *105*, 734.
(37) Stanley, H. E.; Teixeira, J. *J. Chem. Phys.* **1980**, *73*, 3404.

JP911940H